IEEE Access
Multidisciplinary | Rapid Review | Open Access Journal

Received 27 July 2023, accepted 16 August 2023, date of publication 24 August 2023, date of current version 5 September 2023.

Digital Object Identifier 10.1109/ACCESS.2023.3308519

RESEARCH ARTICLE

Unifying the Regional Height System Using Optic-Fiber Clock Network: A Simulation Test for Southeast Asia

ANH THE HOANG[1], ZIYU SHEN[2], AND WEN-BIN SHEN[3,4,5]

[1]School of Agriculture and Natural Resource, Vinh University, Vinh 460000, Vietnam
[2]School of Resources, Environmental Science and Engineering, Hubei University of Science and Technology, Xianning 437100, China
[3]Department of Geophysics, School of Geodesy and Geomatics, Wuhan University, Wuhan 430079, China
[4]Key Laboratory of Geospace Environment and Geodesy, Ministry of Education, Wuhan University, Wuhan 430079, China
[5]State Key Laboratory of Information Engineering in Surveying, Mapping and Remote Sensing, Wuhan University, Wuhan 430079, China

Corresponding author: Ziyu Shen (theorhythm@foxmail.com)

This work was supported by the National Natural Science Foundation of China (NSFC) under Grant 42030105, Grant 42274011, Grant 41721003, and Grant 41874023.

ABSTRACT Orthometric height datum systems are critical in the geodetic community. Nonetheless, individual nations or local regions maintain their distinct height systems. These systems, primarily determined by conventional spirit leveling, exhibit inhomogeneity, as the mean sea level does not represent an equigeopotential surface. As such, accurately unifying global height systems is a persistent challenge. The gravity frequency shift equation provides a promising approach to this issue, offering a means to unify global height systems by comparing the frequencies of two distant clocks via optical fibers. In this study, we develop a model based on the Optical Fiber Frequency Transfer (OFFT) method, recognized for its unparalleled precision. We simulated a network of optical clocks interconnected by optical fibers to unify the height system across Southeast Asia. Our study suggests that the optical fiber clock network can realize height propagation between any two height datums at the centimeter level, providing a favorable opportunity for achieving regional height system unification.

INDEX TERMS Regional height system, optical clocks network, OFFT, gravity frequency shift, frequency transfer, geopotential.

I. INTRODUCTION

Orthometric height (OH) is widespread in scientific and engineering endeavors. The establishment of a uniform global height system is crucial for applications such as studying global sea-level rise, construction of cross-country tunnels, and monitoring of global groundwater levels, among others [1], [2], [3], [4], [5]. Currently, over 100 localized height systems worldwide predominantly rely on classical spirit leveling based on mean sea level. This reliance leads to disparities between these systems, reaching 1-2 meters [1]. To unify the global height system, the International Association of Geodesy (IAG) released two resolutions: resolution No.1 in 2015, for the definition and implementation of the International Altitude Reference System (IHRS), and resolution No.3 in 2019, for the establishment of the International Height Reference Frame (IHRF). Following these resolutions, researchers have proposed various methods to establish a unified global height system [2], [3].

Scientists have studied multiple methodologies to unify the global height system [2], [4], [5], [6], [7]. These include leveling combined with gravity data [2], oceanic leveling [6], estimating the anomalous potential by solving the geodetic boundary value problem [7], and utilizing a global gravity model [8]. However, despite their advantages, these methodologies present significant limitations that inhibit their application in establishing a precise global height system.

Recently, scientists proposed the relativistic geodetic method (RGM) to address this challenge. The RGM is based on Einstein's general relativity theory (GRT) [9]. In GRT, a

The associate editor coordinating the review of this manuscript and approving it for publication was Tianhua Xu.

clock at a point with smaller gravity potential (namely larger orthometric height) runs faster than one at larger gravity potential. Thus, using a precise clock, the height difference between two points can be determined based on the measured time difference between these points. This approach, initially proposed by Bjerhammar [10], is called the clock transport approach (CTA). Another approach uses the gravity frequency shift, which is referred to as the gravity frequency shift approach (GSFA), which determines the height difference between two points after measuring their frequency shift [11], [12]. Both the CTA and GSFA are referred to as the relativistic approach and have been extensively examined and validated by scientists over several decades [4], [5], [12], [13], [14], [15], [16], [17], [18], [19], [20]. To determine the geopotential difference with an accuracy of $0.1\,\mathrm{m}^2/\mathrm{s}^2$ (equivalent to 1 cm in orthometric height), it is required a time (or frequency) measuring system with a stability of 10^{-18}. However, for a long time, the accuracy of clocks was a major barrier to applying the studies of relativistic geodesy into practice. In recent years, atomic optical clocks have obtained great improvements in accuracy, and frequency transfer technique has also made breakthroughs. From 2012 to the present, clocks with a stability of around 10^{-17} to a stability of around 1.0×10^{-18} were successively generated [21], [22], [23], [24], [25], [26], [27], which provide potential applications in geodetic science.

GSFA has been applied to determine the height difference between two points, including clock transport between two points, frequency (time) transmission between two clocks connected by optical fiber, and signal transmission between two stations via GNSS satellite. In those methods, the signal transmission method via fiber optic connection (optical fiber frequency transfer (OFFT) method) can achieve the highest centimeter-level accuracy. Similarly, the satellite frequency signal transmission (SFST) method can achieve altitude determinations with decimeter-to-meter accuracy.

Many researchers have studied their application in geodetic work, recognizing the considerable benefits of optical clock networks [28], [29], [30], [31]. International proposals for potential optical clock networks have emerged, including in Europe [32], the United States [33], and Japan [34]. Some recent proposals envision an optical clock network using fiber optic links to establish an International Height Reference Frame [5], [35], [36], while others propose a similar network with satellite links [4]. These studies underscore the potential of relative geodesy in establishing the global elevation system.

This paper presents a method using frequency signal transmission over optical fiber to determine the height difference between two points. We propose a clock network connected by optical fibers to establish a global height system. Section II elaborates on this proposal. Section III details a simulation experiment designed to test the unification of Southeast Asia's height system using an optical-fiber clock network. The results of the model are presented in Sections IV and the final section will present conclusions and discussions.

II. METHODOLOGY

In this section, we first briefly describe the process of determining the frequency shift between two separate clocks using the OFFT technique and the method of determining the geopotential (as well as the orthometric height) through frequency shift. We then introduce an optic-fiber clock network model that can be used to unify the global height system.

A. GRAVITY FREQUENCY SHIFT EQUATION AND OFFT METHOD

As previously delineated in various studies [4], [11], [36], the GSFA employs the gravity frequency shift equation to ascertain the geopotential difference and the corresponding orthometric height difference between two terrestrial points. Let us assume there is a transmitting station at point A, which emits a frequency of f_A. At point B, a station receives the frequency, denoted as f_B. According to the GRT, there is a correlation between the frequency shift and the geopotential difference between points A and B, as expressed in prior research [10], [11], [12]:

$$\Delta W_{\mathrm{AB}} = -\frac{\Delta f_{\mathrm{AB}}}{f} c^2 + O(c^{-3}) \tag{1}$$

where f is the intrinsic frequency of the clock, which is given; c is the speed of light in vacuum; $\Delta f_{AB} = f_B - f_A$; $\Delta W_{AB} = W_B - W_A$; W_A and W_B are the geopotential at points A and B, respectively, and $O(c^{-3})$ represents the order terms higher than c^{-2}. With small elevation differences (less than 3000 m), Eq. (1) guarantees the accuracy of one-centimeter level. For substantial height differences (more than 3000 m), to attain a centimeter-level precision, it is imperative to utilize a formula that takes high-order terms into account [36].

Equation (1) indicates that once the frequency shift Δf_{AB} is measured, the geopotential difference ΔW_{AB} can be deduced. As mentioned in Section I, OFFT is currently the most accurate method for determining Δf_{AB}, given that frequency transmission via optical fibers can significantly mitigate environmental noise. Several error sources can influence frequency transmission via optical fiber, including the Doppler effect, material dispersion, polarization mode dispersion, fiber nonlinearity effects, and random errors. Methods for mitigating these error sources are detailed in Hoang et al. [36]. For a comprehensive understanding of the OFFT method, readers may refer to relevant literature [36], [37], [38]. However, we will briefly outline the principle of the OFFT method for determining the gravity frequency shift between two stations, A and B.

Let us assume that stations A and B's atomic clock oscillation frequencies are denoted as f_A and f_B, respectively. The frequency signal f_A is transmitted from station A to station B. At station B, the received frequency signal, f'_A, can be expressed as follows:

$$f'_A = (f_{\mathrm{A}} - f_{\mathrm{B}}) + \delta_{clock1} + \delta_{tran1} + \delta_{tide1} + \delta_{planet1} + \delta_{ram1} \tag{2}$$

where δ_{clock1} is the sum of clock errors, including blackbody radiation (BBR), Zeeman effect, etc.; δ_{tran1} is the sum of all frequency transfer process errors, including Doppler effect, the material dispersion, etc.; δ_{tide1} is the error caused by tidal effects; $\delta_{planet1}$ is the sum of errors caused by the principal planets in our solar system, including the Sun, the Moon and other planets (Mercury, Venus, Mars, Jupiter, Saturn, Uranus, Neptune); δ_{ram1} is the random error.

Similarly, frequency signal f_B is transmitted from station B to station A. At station A, the received frequency signal f'_B is:

$$f'_B = (f_B - f_A) + \delta_{clock2} + \delta_{tran2} + \delta_{tide2} + \delta_{planet2} + \delta_{ram2} \quad (3)$$

From Eqs. (2) and (3), we obtain:

$$\begin{aligned} f'_B - f'_A &= (f_B - f_A) - (f_A - f_B) + (\delta_{clock2} - \delta_{clock1}) \\ &\quad + (\delta_{tran2} - \delta_{tran1}) + (\delta_{tide2} - \delta_{tide1}) \\ &\quad + (\delta_{planet2} - \delta_{planet1}) + (\delta_{ram2} - \delta_{ram1}) \\ &= 2\Delta f_{AB} + \delta_{clock} + \delta_{tran} + \delta_{tide} \\ &\quad + \delta_{planet} + \delta_{ram} \end{aligned} \quad (4)$$

where $\Delta f_{AB} = f_B - f_A$; $\delta_{clock} = \delta_{clock2} - \delta_{clock1}$; $\delta_{tran} = \delta_{tran2} - \delta_{tran1}$; $\delta_{tide} = \delta_{tide2} - \delta_{tide1}$; $\delta_{planet} = \delta_{planet2} - \delta_{planet1}$; $\delta_{ram} = \delta_{ram2} - \delta_{ram1}$. Hence, the gravity frequency shift between two stations A and B can be expressed as:

$$\Delta f_{AB} = \frac{f'_B - f'_A}{2} - \frac{\delta_{clock}}{2} - \frac{\delta_{tran}}{2} - \frac{\delta_{tide}}{2} - \frac{\delta_{planet}}{2} - \frac{\delta_{ram}}{2} \quad (5)$$

Then, combining Eqs. (5) and (1), the geopotential difference ΔW_{AB} can be determined.

Let us discuss each term on the right-hand side of Equation (5):

The first term, $f'_B - f'_A$, is the observed frequency shift based on the two-way transmission of optical signals between locations A and B.

The second term, δ_{clock}, accounts for all clock errors. These include errors from blackbody radiation (BBR) [39], [40], the Zeeman effect [40], [41], and the Stark effect [40]. These errors are minimized during the generation of optical atomic clocks, but residual errors (systematic and random) persist. These are termed clock errors and relate to the atomic clock's stability. Two-way signal transmission can eliminate systematic but not random errors, which can be reduced through multiple observations.

The third term, δ_{tran}, refers to the sum of all errors from the frequency transfer process. This term includes the Doppler effect, nonlinear effects, polarization dispersion, and fiber errors. The Doppler effect and fiber errors can be eliminated by two-way techniques during frequency transmission [42]. The fourth term, δ_{tide}, represents the error due to the Earth's deformation from tidal effects. The changes in potential induced by tides can be estimated from global tide models (e.g., [43]) or calculated using specific software [44]. Earth tide effects can reach up to 60 cm [45], but after corrections, residual errors in the vertical direction are on the millimeter scale [46], [47]. The magnitude of the solid earth tide is related to the position. For instance, near the ocean, it is larger, and far away from the ocean, it is smaller. Tide effects must be considered for distant stations (thousands of kilometers apart). If the clock stations are close, two-way techniques can rule out these errors due to identical tidal regimes.

The fifth term, δ_{planet}, is the sum of errors caused by the major planets in the solar system. The positions of these planets can be obtained from the Ephemerides of Planets and the Moon [48]. Similar to tidal effects, planetary influences can be ignored due to two-way observation techniques when the two clock stations are close. However, to achieve centimeter-level accuracy, all celestial bodies (except Neptune) need to be considered for distant stations. After these corrections, residual errors δ_{planet} fall below 1.0×10^{-20} [46].

The sixth term, δ_{ram}, sums up all random errors. This term includes errors from the first and higher-order lattice light shifts, density shifts, line-pulling effects, frequency combs, etc. These errors cannot be eliminated and persist in the measurement results.

Once ΔW_{AB} is determined, we can ascertain the OH of point B if the OH of point A is known, as per Heiskanen and Moritz [49] and Hofmann-Wellenhof and Moritz [50]:

$$H_B = -\frac{\Delta W_{AB} - H_A(g_A + 0.0424 \times H_A)}{g_A + 0.0424 \times H_B^0} \quad (6)$$

where g_A is surface gravity measurement, in gal (cm/s^2), H_B^0 is an approximate orthometric height at point B in km, and ΔW_{AB} is in g.p.u (cm^2/s^2. g.p.u is geopotential unit, 1 g.p.u = 1,000 gal.m). H_B^0 is an approximation that does not affect the final result, as the H_B value will be determined by an iterative process. From Eqs. (1) and (6), we obtain:

$$H_B = \frac{H_A(g_A + 0.0424 \times H_A)}{g_A + 0.0424 \times H_B^0} + \frac{\Delta f_{AB}}{f} c^2 + O(c^{-3}) \quad (7)$$

Eq. (7) shows that given H_A, the H_B can be determined after the gravity frequency shift Δf_{AB} is observed.

B. CLOCK NETWORK FOR UNIFYING THE GLOBAL HEIGHT SYSTEM

We present a novel proposal for an optical clock network to accomplish a unified global height system. In alignment with the IAG convention, the IHRF reference networks must adhere to the hierarchy established by the ITRF. Accordingly, our proposed optical clock network stratifies clocks into three categories: base, master, and slave. This network configuration establishes connections between the various types of clocks through fiber optic frequency transmission. As depicted in Fig. 1, the proposed clock network comprising the master, and slave clocks, interconnected via optical fibers, is designed to harmonize the global or regional height systems. The clocks are distinguished based on their assigned roles within the network: (1) Each country or region has a designated master optical clock station and several subsidiary slave optical clock stations. The master and slave

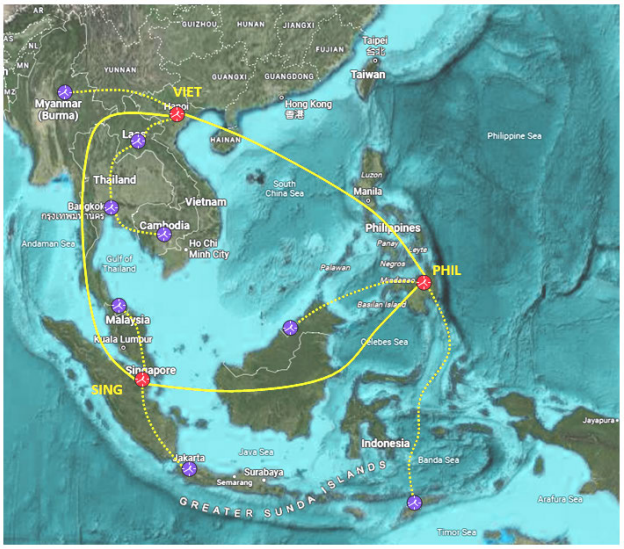

FIGURE 1. Schematic representation of the clock network interlinked through optical fiber frequency transfer methodologies to standardize the Southeast Asia height system. Master clocks, denoted in red, dispersed across different countries or regions, are interconnected via optical fibers, forming a closed loop (yellow solid curve) extending from Vietnam (VIET) to Singapore (SING) to the Philippines (PHIL) and back to Vietnam (VIET). Each master clock is further connected to multiple subordinate clocks (slave clocks), represented in purple, through optical fibers, thereby establishing regional networks (illustrated by dashed yellow curves).

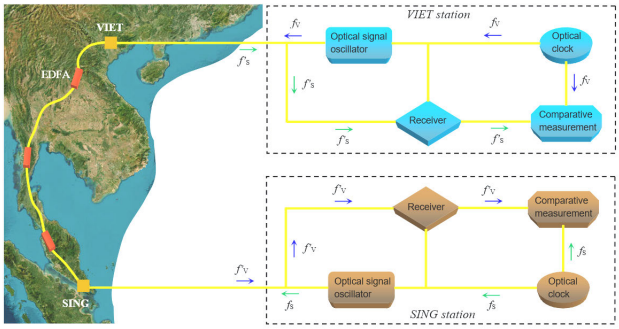

FIGURE 2. Illustration of the connection between the VIET and SING stations, denoted by earth-yellow squares, connected by an optical fiber. The optical fiber incorporates Erbium-doped fiber amplifier (EDFA) devices designed to amplify the signal and guarantee the stable transfer of the frequency signal. f_V and f_S are frequency signals from stations VIET and SING, respectively. f'_V and f'_S are frequency signals obtained at stations SING and VIET, respectively. The signal is transmitted by optical signal oscillators and received by the receiver. The optical signal oscillator and receiver are connected to the optical clock and the comparative measurement device.

clocks are interconnected by optical fibers. (2) The network also incorporates a clock identified as the base clock, which provides a universal reference point for the entire clock system within the network. (3) Master clocks are interconnected via optical fibers through intermediary stations, forming closed loops with at least three clocks in each loop. Each master clock functions as a nodal point in the system. Meanwhile, the placement of slave clocks offers greater flexibility without the requirement of forming a closed loop.

Before practical application, all clocks within the network must undergo a preliminary calibration at a single site. Subsequently, the clocks are strategically positioned at various stations.

III. SIMULATION OF OPTICAL CLOCK NETWORK TO UNIFY THE HEIGHT SYSTEM FOR SOUTHEAST ASIA

To test the viability of employing an optical clock network for unifying the height system, we created a simulation of this network using a fiber-optic link specifically designed for Southeast Asia. This region comprises eleven countries: Indonesia, Malaysia, the Philippines, Singapore, Thailand, Brunei, Cambodia, Laos, Myanmar, Vietnam, and East Timor. Since these nations are predominantly separated by the sea, consisting of several islands and archipelagos (Indonesia and the Philippines), establishing a unified height system presents a challenge.

Most Southeast Asian nations utilize the mean sea level as their initial height data, employing spirit leveling methods to create national height systems. However, using mean sea level as the baseline for height data inevitably results in inconsistencies across the height systems of these countries. Furthermore, the spirit leveling method proves insufficient when the separation between nations is primarily water bodies, making inter-country height system connection a daunting task.

Given these considerations, we propose a fiber-optic optical clock network to streamline the height system across this region. This approach seeks to offer a plausible solution to the geographical and methodological constraints in unifying the height system for Southeast Asia.

We first select three datum stations from the eleven countries under consideration (as indicated in Fig. 1). Each of these countries houses an optical clock station that maintains a connection with one of the three datum stations via optical fiber. The known coordinates of these stations serve as the foundation for our calculations. Leveraging these coordinates and the EGM2008 model, we calculate the geopotential values of the stations, which we regard as the true or model values. Subsequently, we compute the corresponding gravity frequency shifts between any two stations. The subsequent step involves the generation of simulated observations. We introduce various models and random errors to these gravity frequency shifts, enabling us to derive the simulated frequency shifts observed in one-way frequency signal transfer (refer to Table 2 for details). We deduce the gravity frequency shifts from these ''observed'' frequency shifts using a bi-frequency transfer combination. Then we can calculate the geopotential difference between any two stations. Finally, we evaluate our results by comparing the measured geopotential difference with the corresponding EGM2008 model value. This comparison facilitates an assessment of the accuracy of our measured results.

The conceptualization of our simulation proceeds as follows (Fig. 2). Figure 2 shows the connection between the

VIET and SING stations. Optical signal oscillators enable the transmission of signals at each station while receivers handle the reception. Clock signals are converted into optical frequency signals before transmitting via the optical fiber. Upon reception, the optical frequency signal is converted into a microwave frequency signal. Frequency f_V is conveyed from the VIET station to the SING station, with various models and random errors introduced into the signal. As a result, an ''observation'' or measured frequency f'_V is obtained at the SING station. Similarly, frequency f_S is transmitted from the SING station to the VIET station, undergoing the addition of various models and random errors, yielding an ''observation'' f'_S at the VIET station. By amalgamating f'_V and f'_S, the ''measured'' gravity frequency shift is derived, yielding the ''measured'' geopotential difference between the two stations. The accuracy of the measured result can be assessed by comparing the measured geopotential difference with the value calculated from the EGM2008 model. The connections between the SING-PHIL and PHIL-VIET stations operate similarly.

A. INPUT DATA OF THE SIMULATION

To unify the height system across Southeast Asia, we select three datum stations: the VIET station in Vietnam, the SING station in Singapore, and the PHIL station in the Philippines. We consider the data from the VIET station as the source (as shown in Fig. 1).

Employing the coordinates of these three stations and the EGM2008 model [8], we determine the geopotential values W and the gravity values g of these stations. We calculate the orthometric height of the three stations using the formula: $H = h - N$, where h is obtained from the International GNSS Service (IGS) station data available at https://igs.org/network, and the geoid undulation N is computed from the EGM2008 model, accessible from http://icgem.gfz-potsdam.de/calcpoints. We consider these computed values as the true values.

Given the extensive length of the fiber optic connection (exceeding 3000 km), we can establish intermediate stations along the optical fiber between each pair of stations. The optical clocks utilized at these stations are Ca^+-type, boasting stability of 3×10^{-18} [27]. To establish a connection between each pair of these three clocks, we employ single-mode fiber and bidirectional signal transfer to minimize dispersion errors and offset various other errors. Additionally, we incorporate Erbium-doped fiber amplifiers (EDFAs) within the optical fiber to augment the power of the signals. Past experiments [51] have demonstrated the effectiveness of EDFAs in transmitting frequencies over a distance of 920 km, maintaining the stability of 4×10^{-19}.

For our simulation, we allocate an observation time of one hour with a sampling interval of five seconds. In total, we acquire 720 observational values. Table 1 provides detailed information about the clock stations and related parameters of the simulation.

TABLE 1. Relevant parameters used in optical clock network simulation.

Experiment		Values of Parameters
VIET	Coord	21.001^0N, 105.503^0E, 34.8 m
	OH (EGM2008)	62.855
	W	6.263623657306E+07
	g	9.7864499
SING	Coord	1.203^0N, 103.404^0E, 92.5 m
	OH (EGM2008)	85.886
	W	6.263601169723E+07
	g	9.7802897
PHIL	Coord	6.035^0N, 125.075^0E, 121.1 m
	OH (EGM2008)	49.604
	W	6.263636641818E+07
	g	9.7812145
Optical clock		Ca^+ optical clock
Optical fiber		single-mode fiber
Gravity field model		EGM2008
Mearsurement interval		5 s
Observation time length		1 h

B. SIMULATION DATA PROCESSING

From Eq. (1), based on the geopotential values W of two stations: i and j, we can calculate the frequency shift value as follows:

$$\frac{\Delta f_{\mathrm{i\text{-}j}}}{f} = -\frac{W_{\mathrm{j}} - W_{\mathrm{i}}}{c^2} \tag{8}$$

We denote $\Delta f_{(i-j)obs}$ as the simulated observation value. To obtain the value $\Delta f_{(i-j)obs}$, we add the errors to the $\Delta f_{(i-j)}$ value calculated from Eq. (8). In this simulation, we considered various errors sources in the OFFT method [36]: clock errors δ_{clock} (including blackbody radiation effect δ_{BBB}, Zeeman effect δ_{Zee}, Stark effect δ_{Sta}, density shift, line pulling effect, etc.), dispersion error δ_{Dis}, Doppler error δ_{Dop}, fiber nonlinearities errors δ_{Non}, equipment delay errors δ_{delay} and errors originating from the fiber itself δ_{fib}. In addition, the effects of the Earth's tides δ_{tide}, and the influence of planets in the solar system δ_{planet} are also considered. Assessing the magnitude of these errors is crucial in generating observed values, thus rendering the simulation more congruent with reality. The total errors δ_{total} is calculated as follows:

$$\begin{aligned}\delta_{total} = \delta_{clock} + \delta_{Dis} + \delta_{Dop} + \delta_{Non} + \delta_{delay} \\ + \delta_{fib} + \delta_{tide} + \delta_{planet}\end{aligned} \tag{9}$$

As previously stated, we utilize Ca^+-type optical clocks in this simulation, boasting stabilities of 3×10^{-18}, representing some of the most precise timekeeping devices currently available. A detailed enumeration of clock errors is provided in Table 2. The Doppler error δ_{Dop} can be effectively mitigated by applying the Doppler noise cancellation technique [42]. Hence, we consider the Doppler error δ_{Dop} as effectively nullified for this simulation. Similarly, fiber errors δ_{fib} can be eliminated using the two-way frequency transmission technique [42]. In the context of this simulation, where we employ the two-way frequency transmission technique, it is thus reasonable to assume that the fiber errors δ_{fib} are eliminated.

The residual errors are addressed following the methodology outlined by Williams et al. [33]. Utilizing single-mode

TABLE 2. Error magnitudes of different error sources in the simulated OFFT method.

Error sources	Error magnitudes
Blackbody radiation	$\sim 2.7 \times 10^{-18}$ [27]
Zeeman effect	$\sim 1.0 \times 10^{-19}$ [27]
Stark effect	$\sim 1.0 \times 10^{-19}$ [27]
Other effects (density shift, line pulling effect, ect)	$\sim 1.0 \times 10^{-19}$ [27]
Polarization dispersion	$\sim 8.0 \times 10^{-18}$ [33]
Delay effect (including statistical error, frequency combs error, etc.)	$\sim 1.0 \times 10^{-18}$ [36]
Nonlinear effects	$\sim 1.0 \times 10^{-19}$ [27]
Tide effect	$\sim 4.0 \times 10^{-19}$ [46]
Solar system effect	$\sim 1.0 \times 10^{-20}$ [46]
Doppler effect	Removed by using the Doppler noise cancellation technique [42]
Fiber transfer effect	Removed by using a two-way frequency transmission technique [42]
Total errors	$\sim 1.25 \times 10^{-17}$

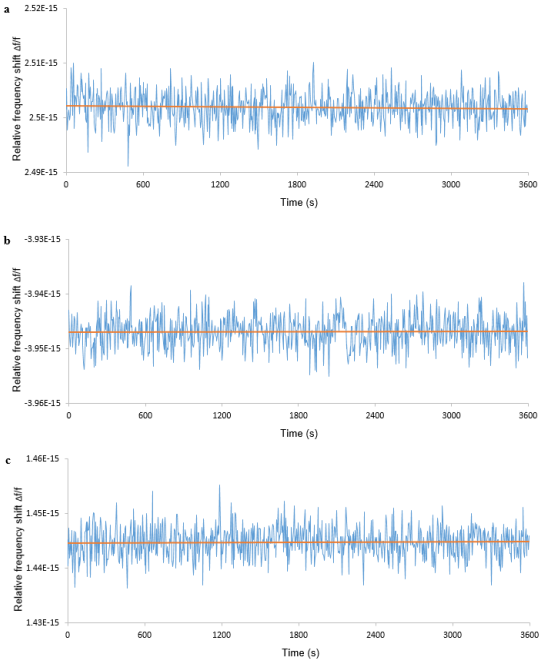

FIGURE 3. Gravity frequency shifts observed between pairs of the three stations (VIET, SING, and PHIL) for one hour, with measurements taken at 5-second intervals, yielding 720 observed values for each station pair. The orange horizontal line represents the mean value. Sub-figure a depicts the data between the VIET and SING stations, sub-figure b presents the data between the SING and PHIL stations, and sub-figure c displays the data between the PHIL and VIET stations.

fiber in the simulation has facilitated mitigating most dispersion errors. The polarization dispersion error is the remaining component with significant influence, with an estimated magnitude of approximately 8.0×10^{-18} [33]. The nonlinear error has been quantified at approximately 8.0×10^{-19}, given a clock laser stability of 8.0×10^{-16} [27]. Delay error has been regulated to remain under 8.0×10^{-18}. The tidal effect is estimated at around 4.0×10^{-19}, while the influence of the planets within our solar system has been assessed to be less than 1.0×10^{-20} [46]. The magnitudes of various errors are enumerated in Table 2.

Upon quantifying the magnitude of these error sources, we conceptualize these errors as noise and subsequently combine them with random noises (white Gaussian noises) to the corresponding true values to generate the simulated observed values. For every station pair, denoted as i and j, two-way measurements are taken: from i to j and vice versa. These measurements yield two observational data series: $\Delta f_{(i-j)obs}$ and $\Delta f_{(j-i)obs}$. Subsequently, the gravity frequency shift value between the two stations is computed using Eq. (10). The results of this computation are presented in Table 3.

$$\Delta f^{g}_{(\mathrm{i\ -\ j})\mathrm{obs}} = \frac{\Delta f_{(\mathrm{i\ -\ j})\mathrm{obs}} - \Delta f_{(\mathrm{j\ -\ i})\mathrm{obs}}}{2} \tag{10}$$

The observed gravity frequency shift values, as acquired for the three pairs of stations under study, are illustrated in Figure 3.

Building upon the observed gravity frequency shift value and utilizing Eq. (1), we can proceed to compute the observed geopotential difference:

$$\Delta W_{(\mathrm{i\ -\ j})\mathrm{obs}} = -\frac{\Delta f^{g}_{(\mathrm{i\ -\ j})\mathrm{obs}}}{f} c^2 \tag{11}$$

Next, the orthometric height of the VIET station (H_{VIET}) can be determined through the application of Eq. (7). This, in turn, enables the calculation of the orthometric heights for both the SING and PHIL stations before circling back to reassess the initial VIET station.

$$\begin{cases} H^{(obs)}_{SING} = -\dfrac{H_{VIET}(g_{VIET} + 0.0424 H_{VIET})}{g_{SING} + 0.0424 H^{0}_{SING}} \\ \qquad\qquad - \dfrac{\Delta W_{(VIET-SING)obs}}{g_{SING} + 0.0424 H^{0}_{SING}} \\ H^{(obs)}_{PHIL} = -\dfrac{H^{(obs)}_{SING}(g_{SING} + 0.0424 H^{(obs)}_{SING})}{g_{PHIL} + 0.0424 H^{0}_{PHIL}} \\ \qquad\qquad - \dfrac{\Delta W_{(SING-PHIL)obs}}{g_{PHIL} + 0.0424 H^{0}_{PHIL}} \\ H^{(obs)}_{VIET} = -\dfrac{H^{(obs)}_{PHIL}(g_{PHIL} + 0.0424 H^{(obs)}_{PHIL})}{g_{VIET} + 0.0424 H^{0}_{VIET}} \\ \qquad\qquad - \dfrac{\Delta W_{(PHIL-VIET)obs}}{g_{VIET} + 0.0424 H^{0}_{VIET}} \end{cases} \tag{12}$$

Utilizing the observed heights, we can derive the discrepancy between these observed values and the true heights calculated from the EGM2008 model as follows:

$$\delta H_{\mathrm{i}} = H^{(obs)}_{\mathrm{i}} - H^{true}_{\mathrm{i}} \tag{13}$$

TABLE 3. Difference between the calculated value using the simulated observations and the corresponding model value (Unit: (m^2/s^2)).

Station	True geopotential difference based on EGM2008	Relative frequency shift $\Delta f/f(\times 10^{-16})$	Calculated geopotential difference	The deviation
VIET-SING	-224.876	25.022 ± 0.021	-224.885 ± 0.185	-0.009 ± 0.185
SING-PHIL	354.721	-39.468 ± 0.020	354.718 ± 0.183	-0.003 ± 0.183
PHIL-VIET	-129.845	14.448 ± 0.022	-129.851 ± 0.202	-0.006 ± 0.202

TABLE 4. Deviation between the orthometric height determined by OFFT using simulated observations and the true value (Unit: m).

Station	True OH based on EGM2008	OH determined by OFFT	The deviatione
VIET	62.855	62.839 ± 0.016	-0.016 ± 0.016
SING	85.886	85.873 ± 0.012	-0.013 ± 0.012
PHIL	49.604	49.634 ± 0.030	0.030 ± 0.030

IV. RESULTS

Eqs. (10) and (11) facilitate deriving the observed gravity frequency shift value and the observed geopotential difference between stations. The disparity between the geopotential difference, based on the optic fiber frequency transfer using the simulated observations, and the genuine geopotential difference derived from the EGM2008 model is demonstrated in Table 3.

From the data presented in Table 3, we compute the orthometric heights of the stations as well as the variance between the observed heights and the actual heights as per the EGM2008 model, according to Eqs. (12) and (13). The outcomes of these calculations are illustrated in Table 4.

The findings indicate that, within a closed loop, the height difference for the VIET station transmitted via the SING and PHIL stations and then reverting to the original VIET station amounted to a discrepancy of approximately 1.6 cm. Errors in the observed values were found to be roughly on the order of centimeters. The results of this simulation further validate that the OFFT method is capable of ascertaining height differences with centimeter-level precision. This level of accuracy substantiates that the OFFT method is currently the most precise methodology within the gravity frequency shift approaches. Consequently, the OFFT method holds considerable potential for unifying the global height system at the centimeter level.

V. DISCUSSION AND CONCLUSION

The challenge of realization of unifying the global height system with centimeter-level accuracy remains an open issue within the geodetic community. Given its superior accuracy, this study proposes using the OFFT method as a viable solution. The global height system could be unified at the centimeter level by implementing an optical clock network equipped with high-performance clocks (1.0×10^{-18} or higher) and connected via optical fibers.

The OFFT method's ability to connect remote stations through intermediate stations renders it an ideal solution for unifying the global height system. Even connecting points separated by oceans is no longer an insurmountable problem. Further enhancing the method's flexibility is the division of clocks into groups of master and slave clocks. Moreover, the utilization of intermediate stations and slave clocks can potentially reduce the overall cost of the method as the accuracy requirements for auxiliary clocks and intermediate stations are less stringent than for the master clocks.

A simulation was established to confirm the fiber-optic optical clock network's accuracy in unifying Southeast Asia's height system. This simulation showcases the method for harmonizing the height system across Southeast Asia, which involves comparing the frequencies of three clocks. The results indicate that the discrepancy between the true orthometric height (OH) as per EGM2008 and the simulated observed OH is either at the centimeter level, with an overall accuracy of the centimeter level. These findings suggest that the OFFT method can potentially unify the global height system with centimeter-level accuracy.

To achieve height determinations at the centimeter level, the accuracy of the clocks should reach a minimum of 1.0×10^{-18}. As clock technology progresses, clocks with an accuracy of 1.0×10^{-19} have been developed in laboratories, while transportable clocks have achieved the 10^{-18} level. This technological advancement boosts the potential applicability and prospect of the OFFT method in unifying the global height system.

Given the widespread availability of the fiber optic cable system worldwide, particularly in urban and residential areas, this existing infrastructure can be utilized to establish a global optical-fiber-clock network. This network could then serve the purpose of unifying the global height system - an accomplishment that could feasibly be realized in the future.

ACKNOWLEDGMENT

The authors would like to thank several reviewers' comments and suggestions, which greatly improved the manuscript.

REFERENCES

[1] M. G. Sideris, "Geodetic world height system unification," *Handbook Geomathematics*, W. Freeden, Z. M. Nashed, and T. Sonar, Eds. Berlin, Germany: Springer, Aug. 2015, pp. 3067–3085.
[2] L. Sánchez and M. Sideris, "Vertical datum unification for the international height reference system (IHRS)," *Geophys. J. Int.*, vol. 209, no. 2, pp. 570–586, 2017.
[3] J. Ihde, L. Sánchez, R. Barzaghi, H. Drewes, C. Foerste, T. Gruber, G. Liebsch, U. Marti, R. Pail, and M. Sideris, "Definition and proposed realization of the international height reference system (IHRS)," *Surv. Geophys.*, vol. 38, no. 3, pp. 549–570, May 2017.
[4] Z. Shen, W. Shen, S. Zhang, C. K. Shum, T. Zhang, L. He, Z. Cai, S. Xiong, and L. X. Wang, "Unification of a global height system at the centimeter-level using precise clock frequency signal links," *Remote Sens.*, vol. 15, no. 12, p. 2030, Jun. 2023.

[5] H. Wu and J. Müller, *Towards an International Height Reference Frame Using Clock Networks*. Berlin, Germany: Springer, 2020.

[6] E. Stöcker-Meier, "Theory of oceanic levelling for improving the geoid from satellite altimetry," *Bulletin géodésique*, vol. 64, pp. 247–258, Sep. 1990.

[7] R. Rummel and P. Teunissen, "Height datum definition, height datum connection and the role of the geodetic boundary value problem," *Bull. Géodésique*, vol. 62, no. 4, pp. 477–498, Dec. 1988.

[8] N. K. Pavlis, S. A. Holmes, S. C. Kenyon, and J. K. Factor, "The development and evaluation of the Earth Gravitational Model 2008 (EGM2008)," *J. Geophys. Res. Solid Earth*, vol. 62, no. 4, pp. 477–498, 1988.

[9] A. Einstein, "Die Feldgleichungen der Gravitation," in *Sitzungsberichte der Königlich Preußischen Akademie der Wissenschaften*. Berlin, Germany, 1915, pp. 844–847.

[10] A. Bjerhammar, "On a relativistic geodesy," *Bull. Géodésique*, vol. 59, no. 3, pp. 207–220, Sep. 1985.

[11] W. Shen, D. Chao, and B. Jin, "Determination of the geopotential and orthometric height based on frequency shift equation," *Natural Sci.*, vol. 3, no. 5, pp. 388–396, 2011.

[12] W. Shen, D. Chao, and J. Liu, "On the relativistic geoid," *Boll. di Geod. e Sci. Affin.*, vol. 52, no. 3, pp. 207–216, 1993.

[13] R. V. Pound and G. A. Rebka, "Gravitational red-shift in nuclear resonance," *Phys. Rev. Lett.*, vol. 3, no. 9, pp. 439–441, Nov. 1959.

[14] J. L. Snider, "New measurement of the solar gravitational red shift," *Phys. Rev. Lett.*, vol. 28, no. 13, pp. 853–856, Mar. 1972.

[15] T. Katila and K. J. Riski, "Measurement of the interaction between electromagnetic radiation and gravitational field using ^{67}Zn Mössbauer spectroscopy," *Phys. Lett. A*, vol. 83, no. 2, pp. 51–54, May 1981.

[16] M. Vermeer, "Chronometric levelling," Geodetiska Institutet, Suomen Geodeettinen laitos, Masala, Finland, Tech. Rep. 83:2, 1983.

[17] C. Lisdat et al., "A clock network for geodesy and fundamental science," *Nature Commun.*, vol. 7, p. 12443, Aug. 2016.

[18] J. Grotti et al., "Geodesy and metrology with a transportable optical clock," *Nature Phys.*, vol. 14, no. 5, pp. 437–441, May 2018.

[19] M. Takamoto, I. Ushijima, N. Ohmae, T. Yahagi, K. Kokado, H. Shinkai, and H. Katori, "Test of general relativity by a pair of transportable optical lattice clocks," *Nature Photon.*, vol. 14, pp. 411–415, Apr. 2020.

[20] Y. Wu and W.-B. Shen, "Simulation experiments on high-precision VGOS time transfer for future geopotential difference determination," *Adv. Space Res.*, vol. 68, no. 6, pp. 2453–2469, Sep. 2021.

[21] S. Falke, N. Lemke, C. Grebing, B. Lipphardt, S. Weyers, V. Gerginov, N. Huntemann, C. Hagemann, A. Al-Masoudi, S. Häfner, S. Vogt, U. Sterr, and C. Lisdat, "A strontium lattice clock with 3×10^{-17} inaccuracy and its frequency," *New J. Phys.*, vol. 16, no. 7, Jul. 2014, Art. no. 073023.

[22] T. L. Nicholson, S. L. Campbell, R. B. Hutson, G. E. Marti, B. J. Bloom, R. L. McNally, W. Zhang, M. D. Barrett, M. S. Safronova, G. F. Strouse, W. L. Tew, and J. Ye, "Systematic evaluation of an atomic clock at 2×10^{-18} total uncertainty," *Nature Commun.*, vol. 6, no. 1, p. 6896, Apr. 2015.

[23] N. Huntemann, C. Sanner, B. Lipphardt, C. Tamm, and E. Peik, "Single-ion atomic clock with 3×10^{-18} systematic uncertainty," *Phys. Rev. Lett.*, vol. 116, no. 6, Feb. 2016, Art. no. 063001.

[24] W. F. McGrew, X. Zhang, R. J. Fasano, S. A. Schäffer, K. Beloy, D. Nicolodi, R. C. Brown, N. Hinkley, G. Milani, M. Schioppo, T. H. Yoon, and A. D. Ludlow, "Atomic clock performance enabling geodesy below the centimetre level," *Nature*, vol. 564, no. 7734, pp. 87–90, Nov. 2018.

[25] M. Pizzocaro, F. Bregolin, P. Barbieri, B. Rauf, F. Levi, and D. Calonico, "Absolute frequency measurement of the $^1S_0$–$^3P_0$ transition of ^{171}Yb with a link to international atomic time," *Metrologia*, vol. 57, no. 3, May 2020, Art. no. 035007.

[26] K. Beloy, M. I. Bodine, and T. T. Bothwell, "Frequency ratio measurements at 18-digit accuracy using an optical clock network," *Nature*, vol. 591, no. 7851, pp. 564–569, Mar. 2021.

[27] H. Yao, Z. Baolin, and Z. T. Mengyan, "Liquid nitrogen-cooled Ca^+ optical clock with systematic uncertainty of 3×10^{-18}," *Phys. Rev. Appl.*, vol. 17, no. 3, Mar. 2022, Art. no. 034041.

[28] T. Takano, M. Takamoto, I. Ushijima, N. Ohmae, T. Akatsuka, A. Yamaguchi, Y. Kuroishi, H. Munekane, B. Miyahara, and H. Katori, "Geopotential measurements with synchronously linked optical lattice clocks," *Nature Photon.*, vol. 10, no. 10, pp. 662–666, Oct. 2016.

[29] Y. Huang, H. Zhang, and B. T. Zhang, "Geopotential measurement with a robust, transportable Ca^+ optical clock," *Phys. Rev. A, Gen. Phys.*, vol. 102, no. 5, Nov. 2020, Art. no. 050802.

[30] H. Wu, J. Müller, and C. Lämmerzahl, "Clock networks for height system unification: A simulation study," *Geophys. J. Int.*, vol. 216, no. 3, pp. 1594–1607, Mar. 2019.

[31] A. T. Hoang, Z. Shen, K. Wu, A. Ning, and W. Shen, "Test of determining geopotential difference between two sites at Wuhan based on optical clocks' frequency comparisons," *Remote Sens.*, vol. 14, no. 19, p. 4850, Sep. 2022.

[32] F. Riehle, "Optical clock networks," *Nature Photon.*, vol. 11, no. 1, pp. 25–31, Jan. 2017.

[33] P. A. Williams, W. C. Swann, and N. R. Newbury, "High-stability transfer of an optical frequency over long fiber-optic links," *J. Opt. Soc. Amer. B, Opt. Phys.*, vol. 125, no. 8, pp. 1284–1293, Jul. 2008.

[34] T. Akatsuka, H. Ono, K. Hayashida, K. Araki, M. Takamoto, T. Takano, and H. Katori, "30-km-long optical fiber link at 1397 nm for frequency comparison between distant strontium optical lattice clocks," *Jpn. J. Appl. Phys.*, vol. 53, no. 3, Feb. 2014, Art. no. 032801.

[35] A. T. Hoang and W. B. Shen, "Optic-fiber gravity frequency transfer network," in *Proc. 23rd EGU Gen. Assem.*, Apr. 2021, pp. 19–30.

[36] A. T. Hoang, Z. Shen, W. Shen, C. Cai, W. Xu, A. Ning, and Y. Wu, "Determination of the orthometric height difference based on optical fiber frequency transfer technique," *Geodesy Geodyn.*, vol. 12, no. 6, pp. 405–412, Nov. 2021.

[37] W.-B. Shen, "Orthometric height determination based upon optical clocks and fiber frequency transfer technique," in *Proc. Saudi Int. Electron., Commun. Photon. Conf.*, Apr. 2013, pp. 1–4.

[38] Z. Shen, W.-B. Shen, Z. Peng, T. Liu, S. Zhang, and D. Chao, "Formulation of determining the gravity potential difference using ultra-high precise clocks via optical fiber frequency transfer technique," *J. Earth Sci.*, vol. 30, no. 2, pp. 422–428, Apr. 2019.

[39] M. S. Safronova, M. G. Kozlov, and C. W. Clark, "Blackbody radiation shifts in optical atomic clocks," *IEEE Trans. Ultrason., Ferroelectr., Freq. Control*, vol. 59, no. 3, pp. 439–447, Mar. 2012.

[40] N. Poli, C. W. Oates, P. Gill, and G. M. Tino, "Optical atomic clocks," *Rivista del Nuovo Cimento*, vol. 36, no. 12, pp. 555–624, 2014.

[41] Q. Gao, M. Zhou, C. Han, S. Li, S. Zhang, Y. Yao, B. Li, H. Qiao, D. Ai, G. Lou, M. Zhang, Y. Jiang, Z. Bi, L. Ma, and X. Xu, "Systematic evaluation of a ^{171}Yb optical clock by synchronous comparison between two lattice systems," *Sci. Rep.*, vol. 8, no. 1, p. 8022, May 2018.

[42] D. Calonico, E. K. Bertacco, C. E. Calosso, C. Clivati, G. A. Costanzo, M. Frittelli, A. Godone, A. Mura, N. Poli, D. V. Sutyrin, G. Tino, M. E. Zucco, and F. Levi, "High-accuracy coherent optical frequency transfer over a doubled 642-km fiber link," *Appl. Phys. B, Lasers Opt.*, vol. 117, no. 3, pp. 979–986, Dec. 2014.

[43] M. E. Parke, "O1, P1, N2 models of the global ocean tide on an elastic earth plus surface potential and spherical harmonic decompositions for M2, S2, and K1," *Mar. Geodesy*, vol. 6, no. 1, pp. 35–81, Jan. 1982.

[44] M. Van Camp and P. Vauterin, "Tsoft: Graphical and interactive software for the analysis of time series and earth tides," *Comput. Geosci.*, vol. 31, no. 5, pp. 631–640, Jun. 2005.

[45] M. Poutanen, M. Vermeer, and J. Mäkinen, "The permanent tide in GPS positioning," *J. Geodesy*, vol. 70, no. 8, pp. 499–504, May 1996.

[46] Z. Shen, W.-B. Shen, and S. Zhang, "Determination of gravitational potential at ground using optical-atomic clocks on board satellites and on ground stations and relevant simulation experiments," *Surv. Geophys.*, vol. 38, no. 4, pp. 757–780, Jul. 2017.

[47] F. Li, J. Lei, S. Zhang, C. Ma, W. Hao, E. Dongchen, and Q. Zhang, "The impact of solid Earth-tide model error on tropospheric zenith delay estimates and GPS coordinate time series," *Surv. Rev.*, vol. 50, no. 361, pp. 355–363, Jul. 2018.

[48] E. V. Pitjeva, "Updated IAA RAS planetary ephemerides-EPM2011 and their use in scientific research," *Sol. Syst. Res.*, vol. 47, no. 5, pp. 386–402, Sep. 2013.

[49] W. A. Heiskanen and H. Moritz, "Physical geodesy," *Bull. Géodésique*, vol. 86, no. 1, pp. 491–492, Dec. 1967.

[50] B. Hofmann-Wellenhof and H. Moritz, *Physical Geodesy*. Cham, Switzerland: Springer, 2005.

[51] K. Predehl, G. Grosche, S. M. F. Raupach, S. Droste, O. Terra, J. Alnis, T. Legero, T. W. Hänsch, T. Udem, R. Holzwarth, and H. Schnatz, "A 920-kilometer optical fiber link for frequency metrology at the 19th decimal place," *Science*, vol. 336, no. 6080, pp. 441–444, Apr. 2012.